Electronic Supplementary Information (ESI)

Cationic first-row transition metal saccharinate complexes with tris(2-pyridylmethyl)amine: Synthesis, structures and anticancer studies

Ceyda Icsel [a,*], Şeyma Aydinlik [b], Muhittin Aygun [c], Veysel T. Yilmaz [a]

[a] Department of Chemistry, Faculty of Science, Karadeniz Technical University, 61080 Trabzon, Turkey
[b] TUBITAK Marmara Research Center, Climate and Life Sciences, Biotechnology Research Group, 41470 Gebze, Kocaeli, Turkey
[c] Department of Physics, Faculty of Sciences, Dokuz Eylul University, 35210 Izmir, Turkey

Corresponding Author:
Assoc. Prof. Dr. Ceyda Icsel
Department of Chemistry
Karadeniz Technical University
61080 Trabzon, Turkey

E-mail address: cydyilmaz@ktu.edu.tr (C. Icsel)

Table S1 Crystallographic data and structure refinement for **Fe**, **Ni** and **Cu**

	Fe	**Ni**	**Cu**
Empirical formula	$C_{50}H_{50}Cl_2Fe_2N_{10}O_{10}S_2$	$C_{32}H_{34}N_6NiO_{10}S_2$	$C_{32}H_{26}CuN_6O_6S_2$
Formula weight	1197.72	785.48	718.25
Crystal system	Triclinic	Monoclinic	Triclinic
Space group	$P\bar{1}$	$P2_1$	$P\bar{1}$
a (Å)	18.776(8)	10.148(2)	10.5153(9)
b (Å)	19.465(7)	16.206(3)	12.5550(11)
c (Å)	19.694(6)	10.515(2)	13.0375(14)
α (°)	99.02(3)	90	62.831(10)
β (°)	112.39(3)	94.258(16)	80.017(8)
γ (°)	116.69(4)	90	84.164 (7)
V (Å^3)	5457(4)	1724.5(5)	1507.6 (3)
T (K)	295(2)	295(2)	295(2)
Z	4	2	2
ρ_{calc} (g cm^{-3})	1.458	1.513	1.582
μ (mm^{-1})	0.772	0.75	0.921
F(000)	2472	816	738
θ (º)	3.061–25.105	2.971–25.027	3.182–25.027
Collected refls	32405	6532	8356
Data/parameters	10907/897	4420/470	5295/424
Goodness-of-fit	0.974	0.991	1.031
R_1 [$I>2\sigma$]	0.124	0.052	0.056
wR_2	0.384	0.084	0.112

Table S2 Hydrogen bond geometry (Å, º) in **Fe** and **Ni**[a]

D–H···A	D–H (Å)	H···A (Å)	D···A (Å)	D–H···A (º)
Fe				
O1W—H1WA···O2	0.85	2.19	2.78 (3)	127
O1W—H1WB···O2W	0.85	2.09	2.80 (3)	141
O2W—H2WA···O4W^{i}	0.85	2.39	2.84 (3)	114
O2W—H2WB···O7^{ii}	0.85	2.16	2.93 (3)	149
O3W—H3WA···O5	0.85	2.15	2.80 (3)	133
O3W—H3WB···O4W	0.85	1.98	2.80 (3)	162
O4W—H4WA···O2W^{i}	0.85	2.32	2.84 (3)	120
O4W—H4WB···O11^{iii}	0.85	2.58	2.95 (3)	107
O5W—H5WA···O13	0.85	2.26	2.93 (3)	135
O5W—H5WB···O3W	0.85	1.94	2.72 (3)	154
O6W—H6WA···O11	0.85	2.53	3.21 (3)	138
O6W—H6WB···N5^{iv}	0.85	2.31	3.02 (3)	141
Ni				
O1W—H1WA···N5	0.85	1.87	2.691 (8)	161
O1W—H1WB···O5	0.85	1.94	2.785 (7)	173
O2W—H2WA···O3W	0.85	1.86	2.706 (10)	170
O2W—H2WB···N6	0.85	2.00	2.818 (9)	162
O3W—H3WA···O4^{v}	0.85	1.97	2.812 (10)	174
O3W—H3WB···O1	0.85	2.05	2.867 (9)	162
O4W—H4WA···O1^{vi}	0.85	2.30	2.862 (11)	124
O4W—H4WB···O4	0.85	2.08	2.865 (10)	153

[a] Symmetry codes: (i) −*x*+1, −*y*, −*z*+1; (ii) *x*+1, *y*, *z*; (iii) −*x*+1, −*y*+1, −*z*+1; (iv) *x*, *y*+1, *z*.; (v) −*x*+1, *y*−1/2, −*z*+2; (vi) −*x*+1, *y*+1/2, −*z*+2.

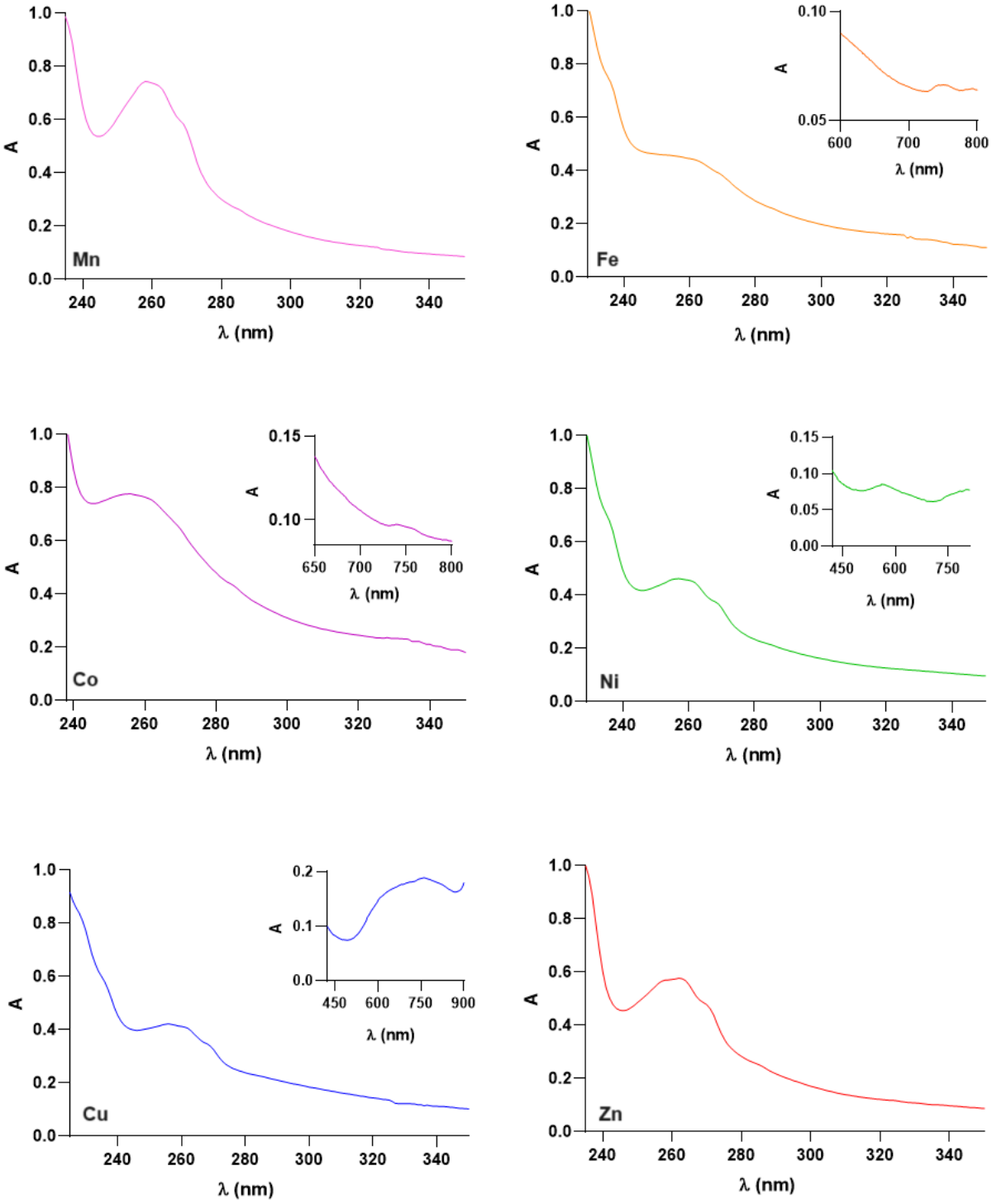

Fig. S1 UV-Vis spectra of metal sac complexes of tpma in MeOH (10 µM).

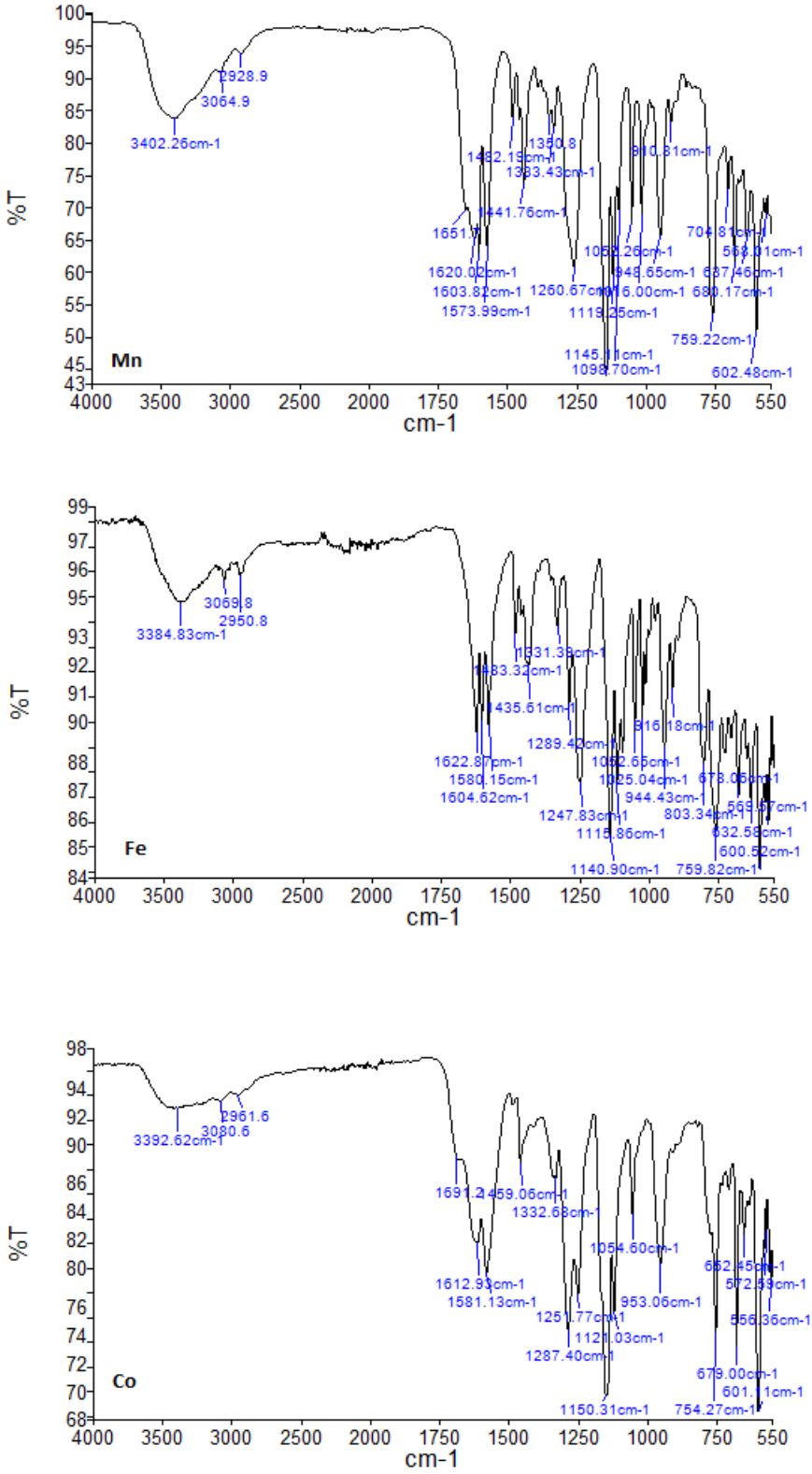

Fig. S2 continued

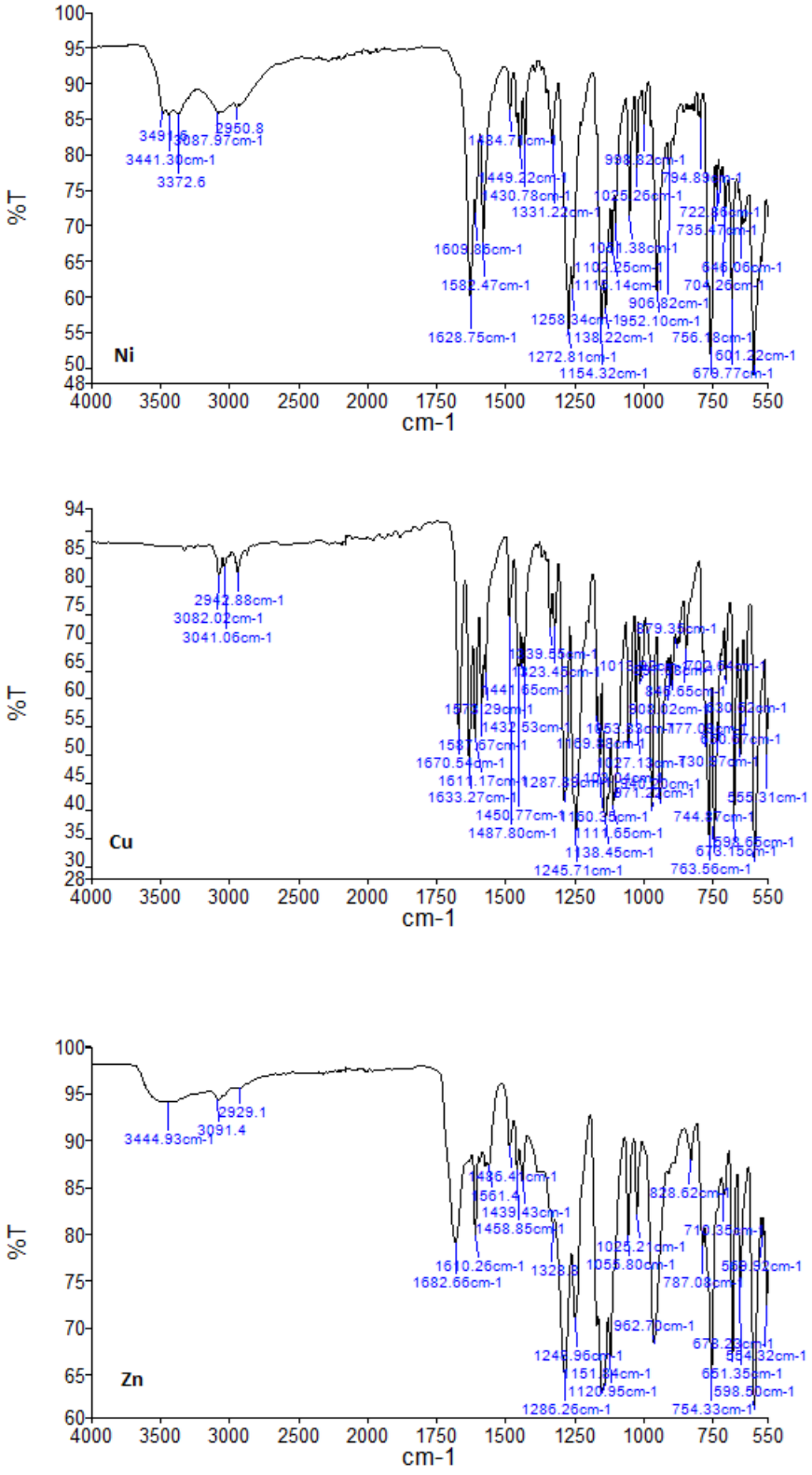

Fig. S2 IR spectra of metal sac complexes of tpma.

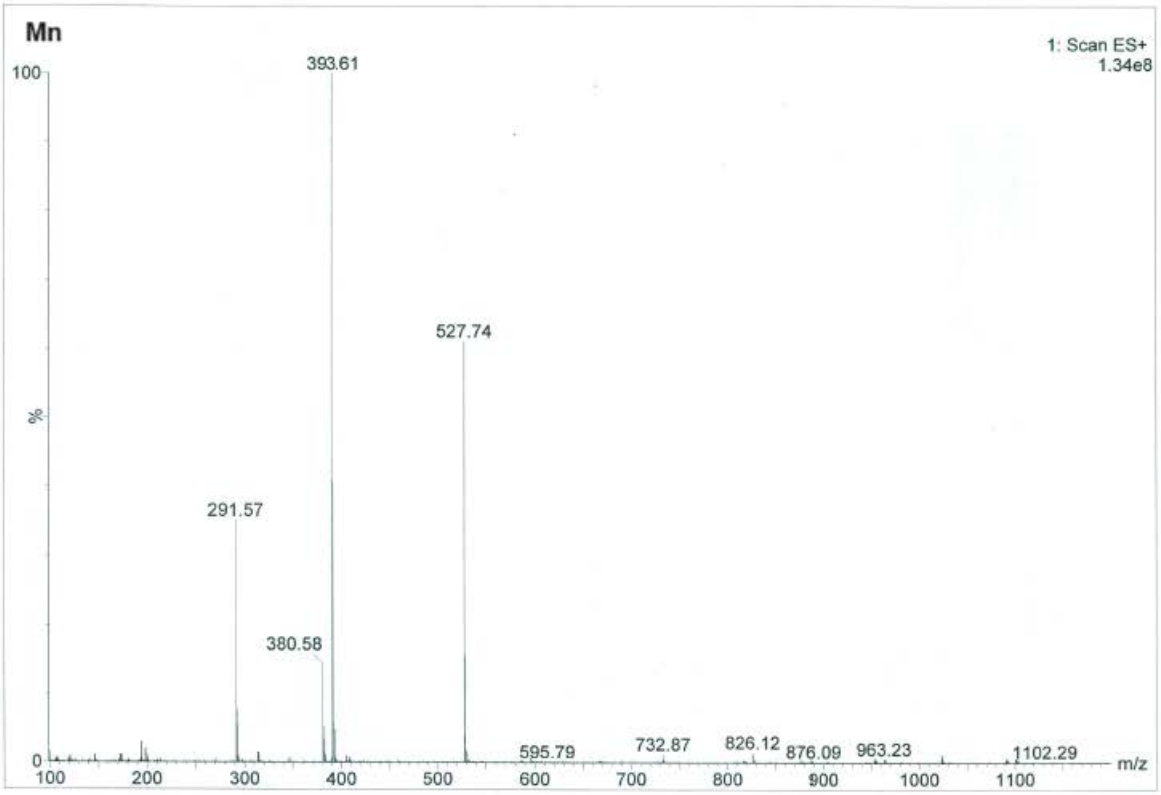

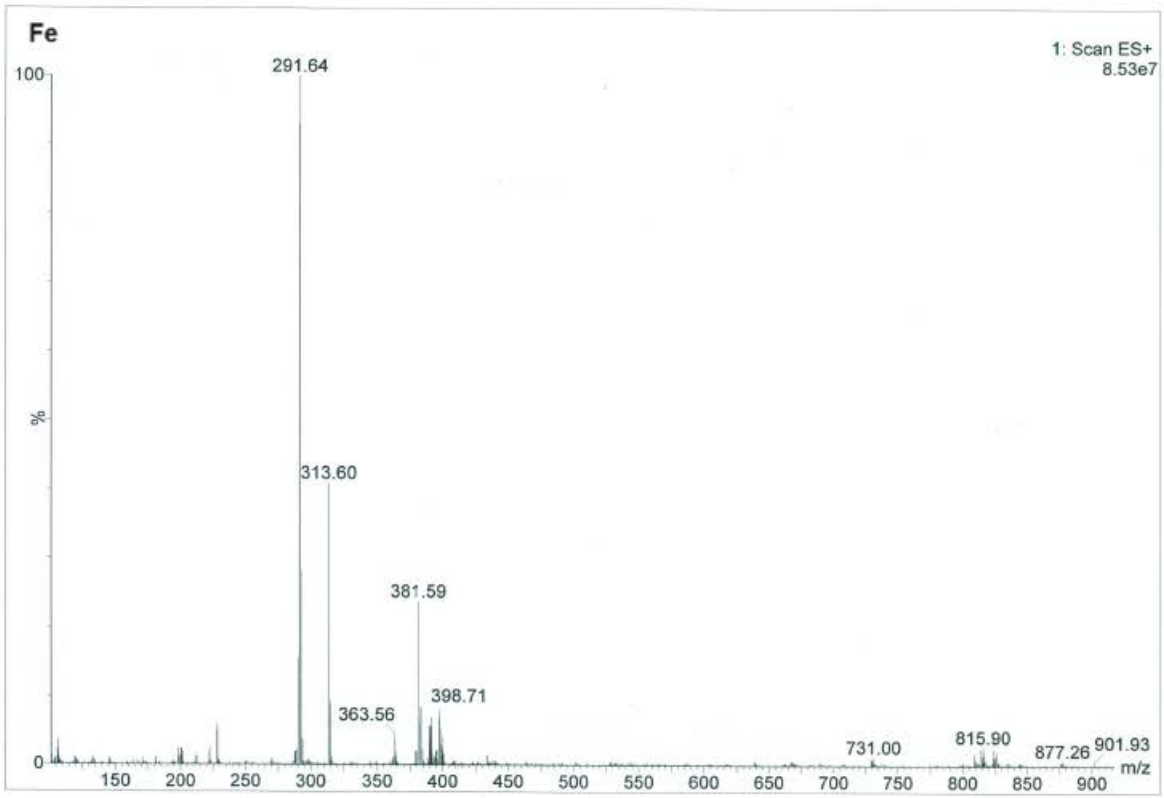

Fig. S3 continued

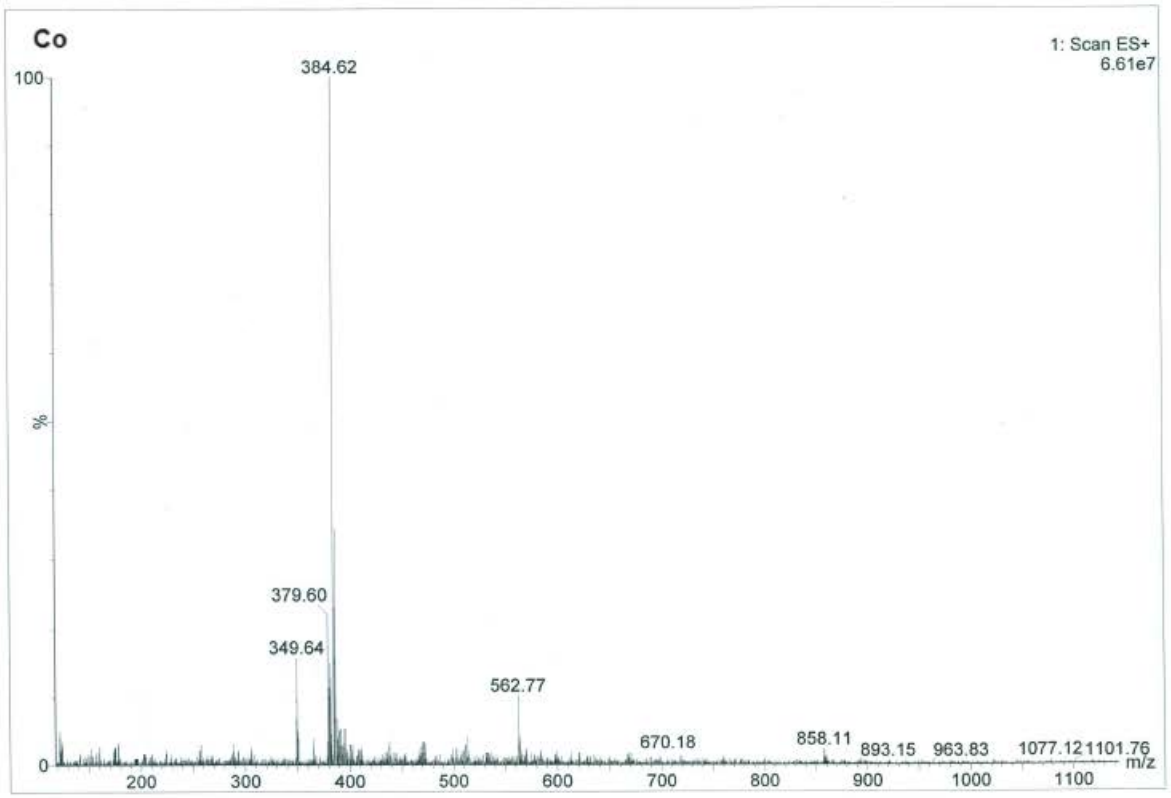

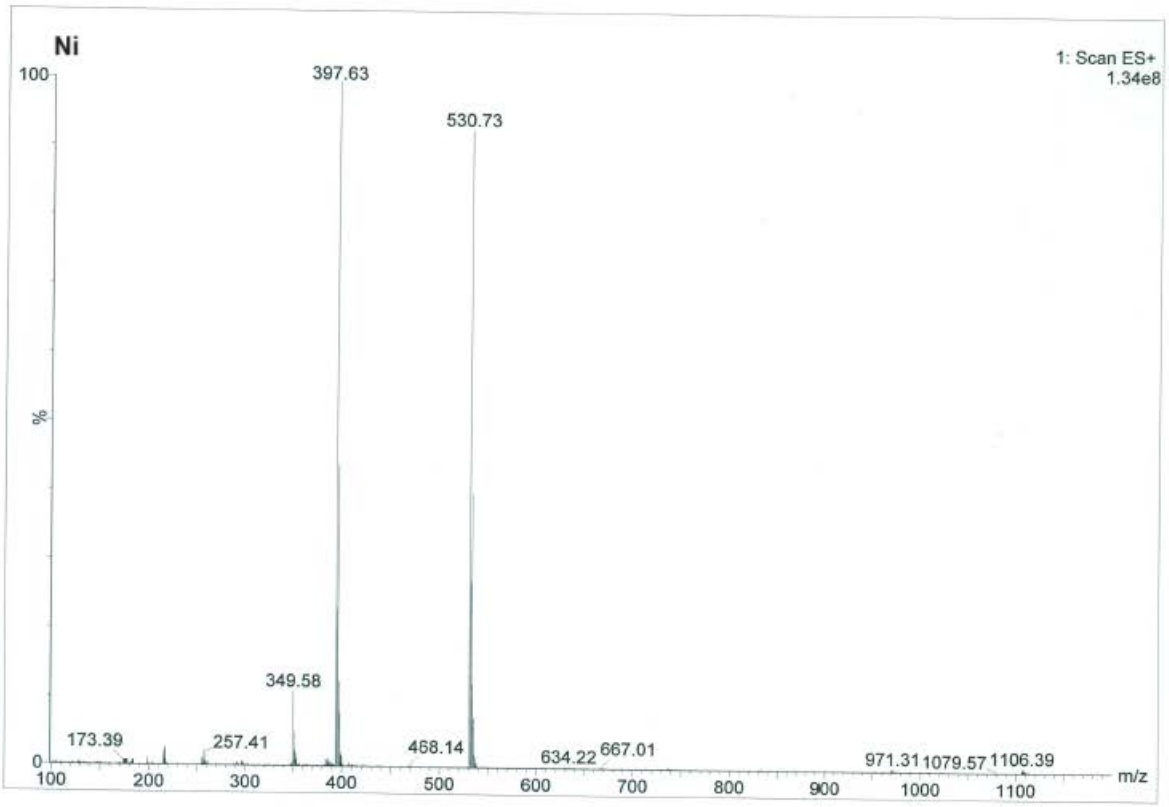

Fig. S3 continued

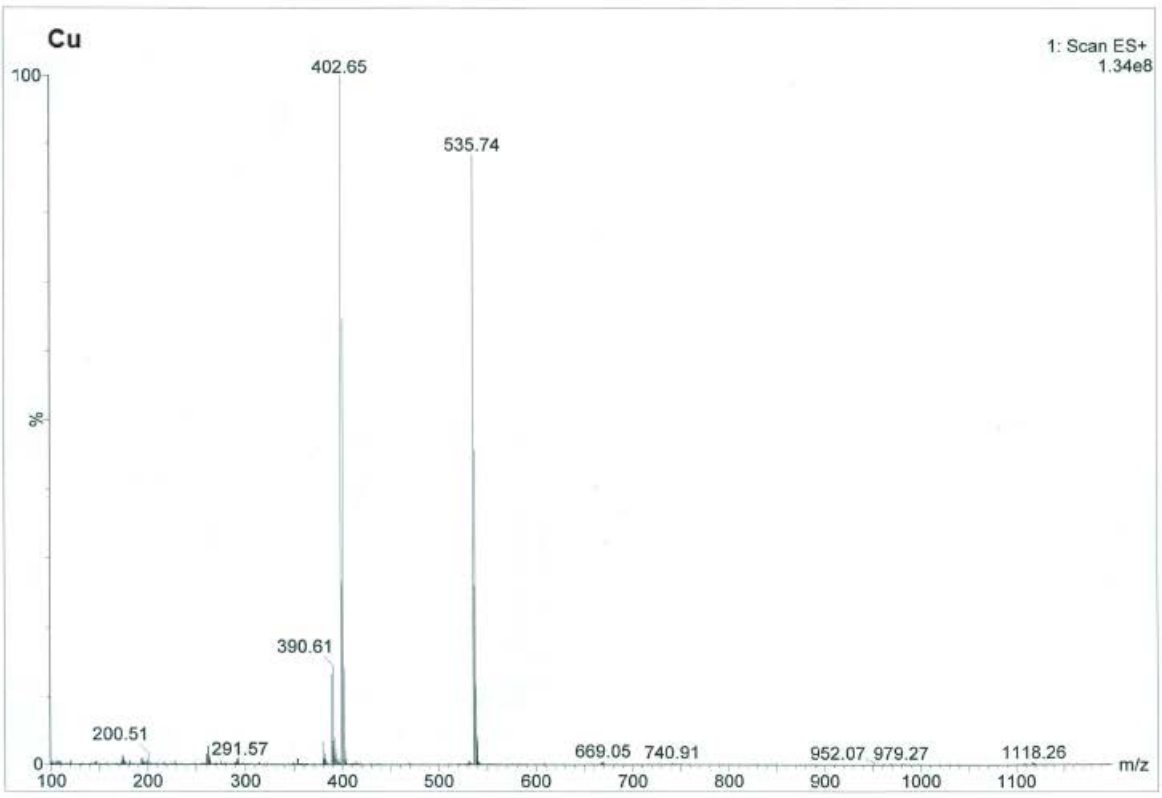

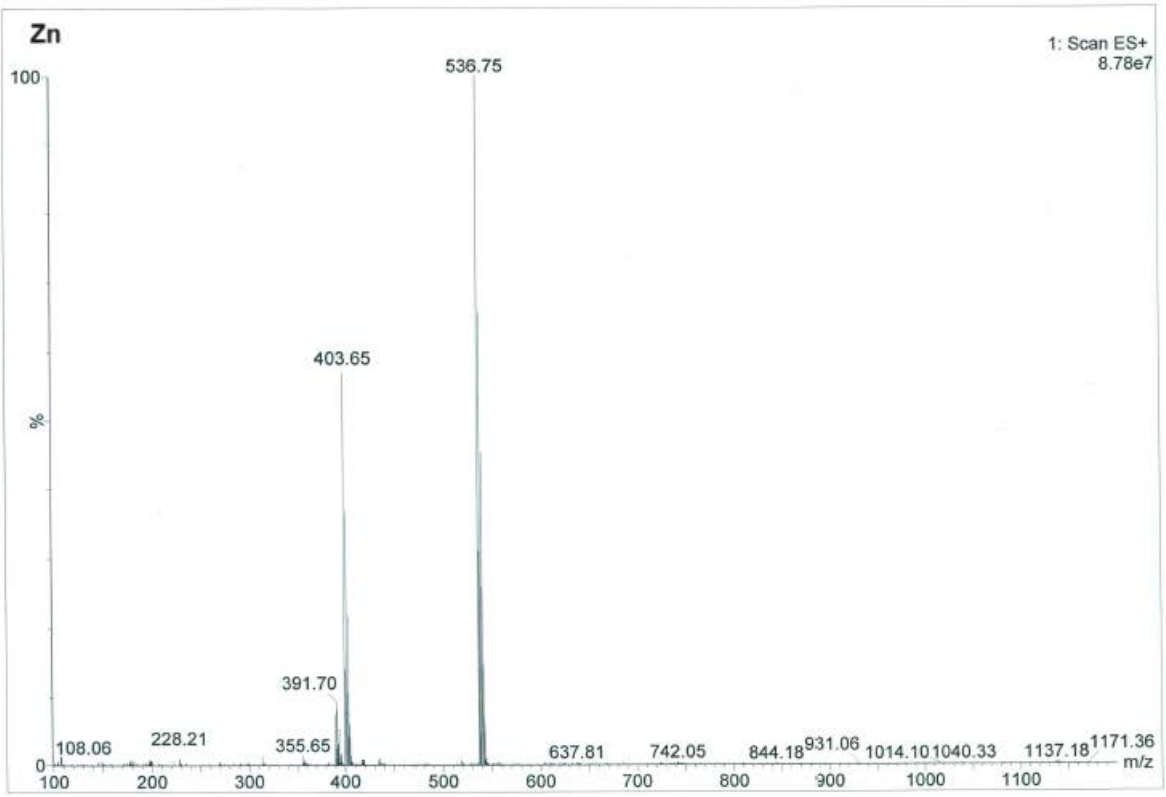

Fig. S3 ESI-MS spectra of metal sac complexes of tpma.

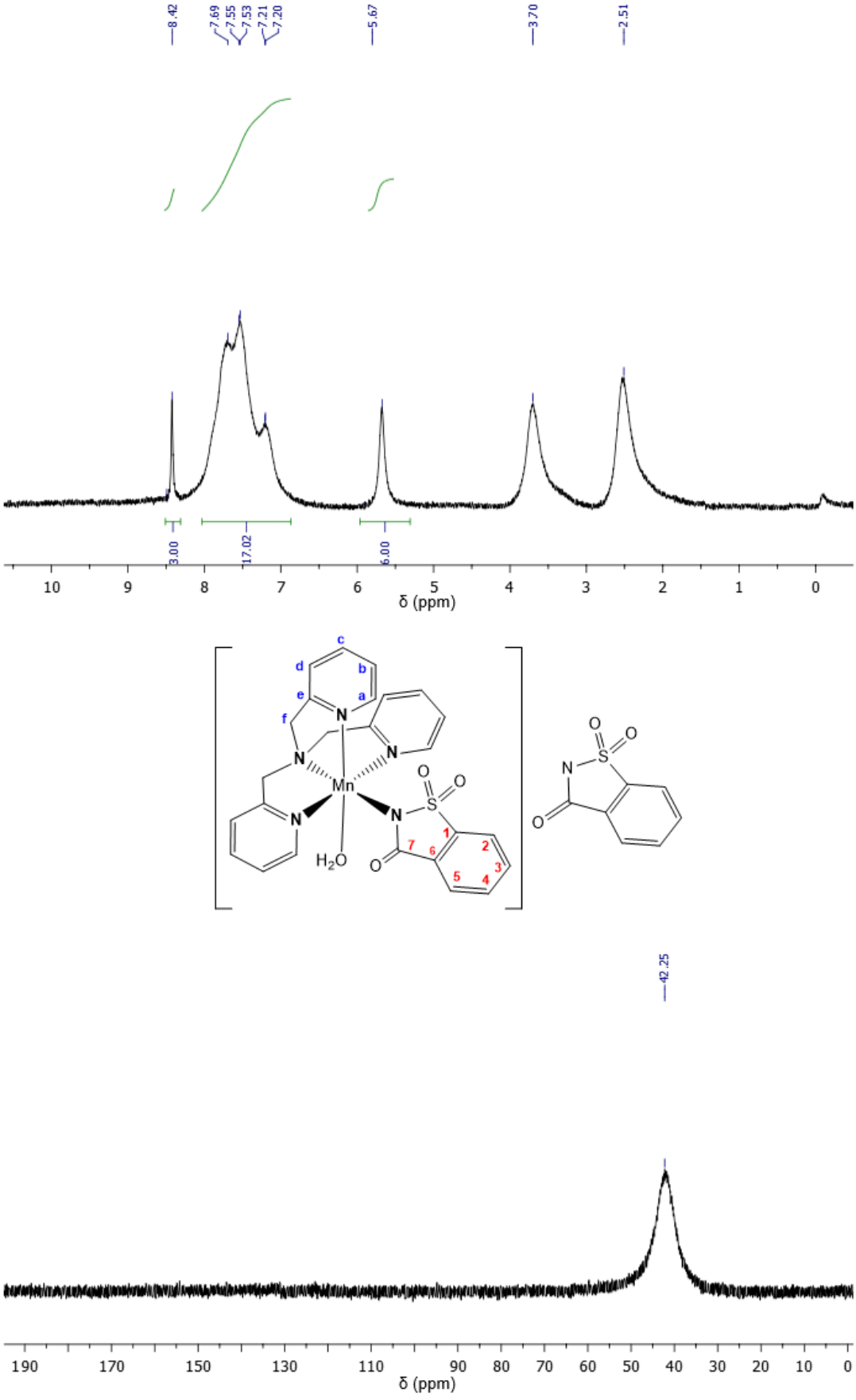

Fig. S4 continued

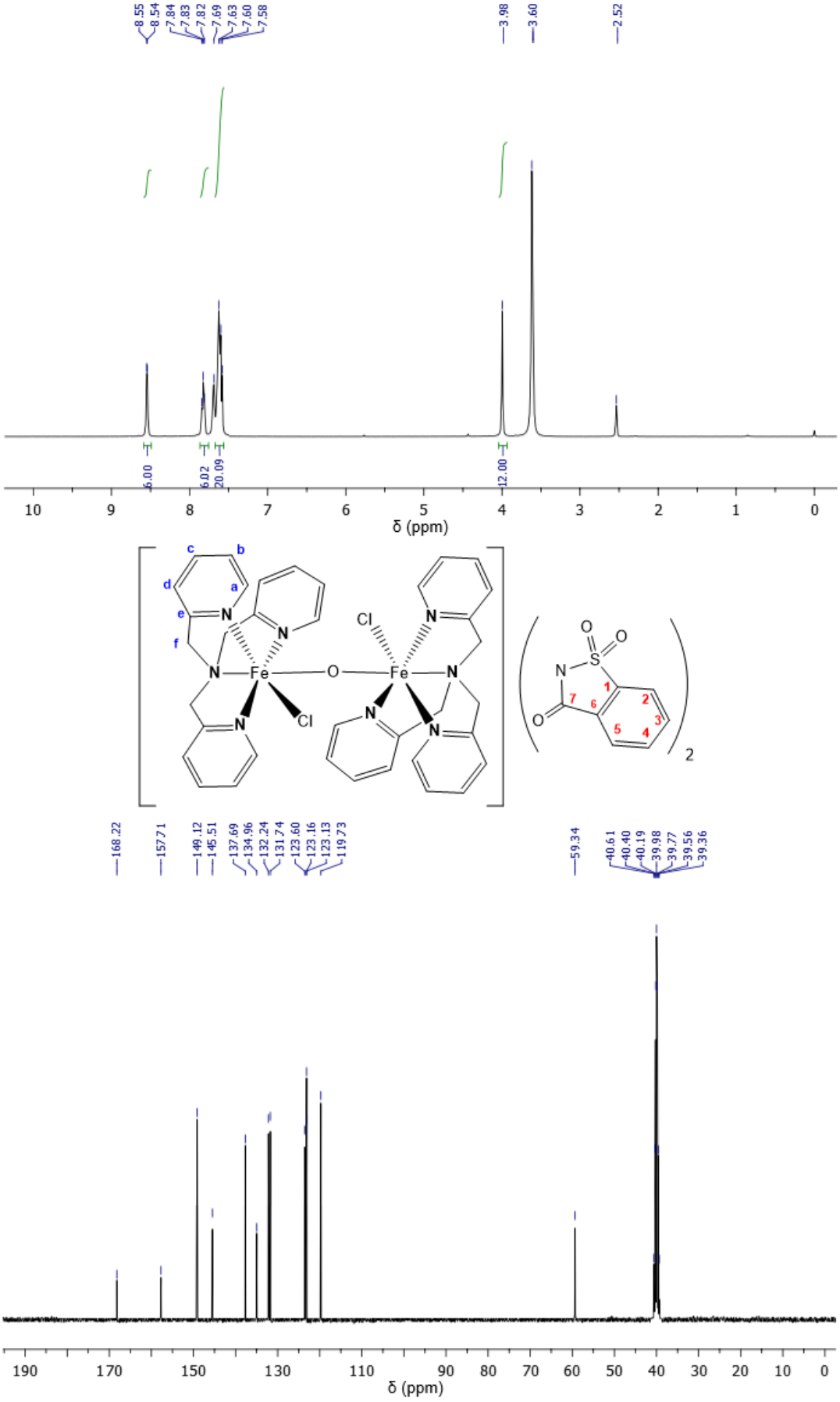

Fig. S4 continued

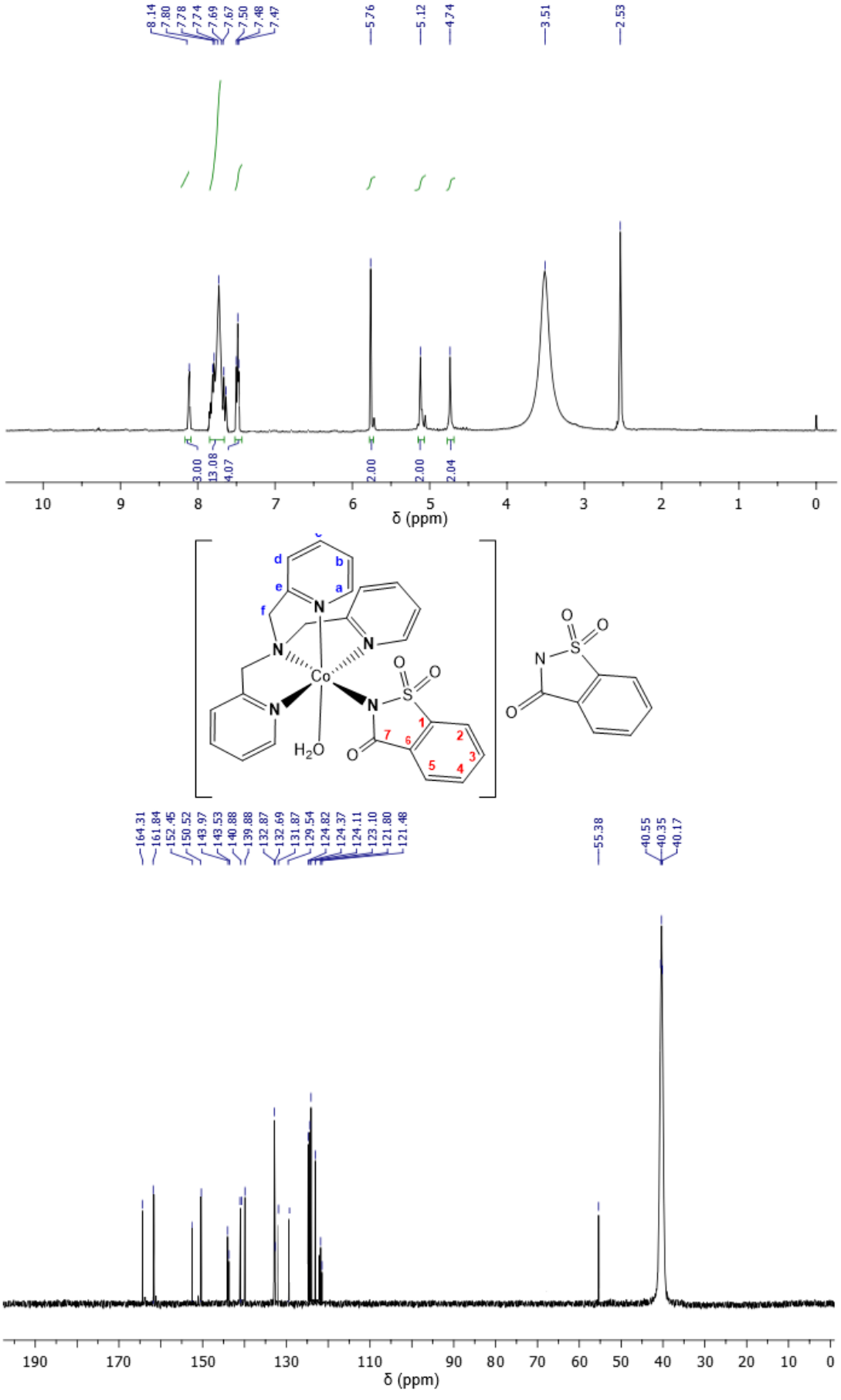

Fig. S4 continued

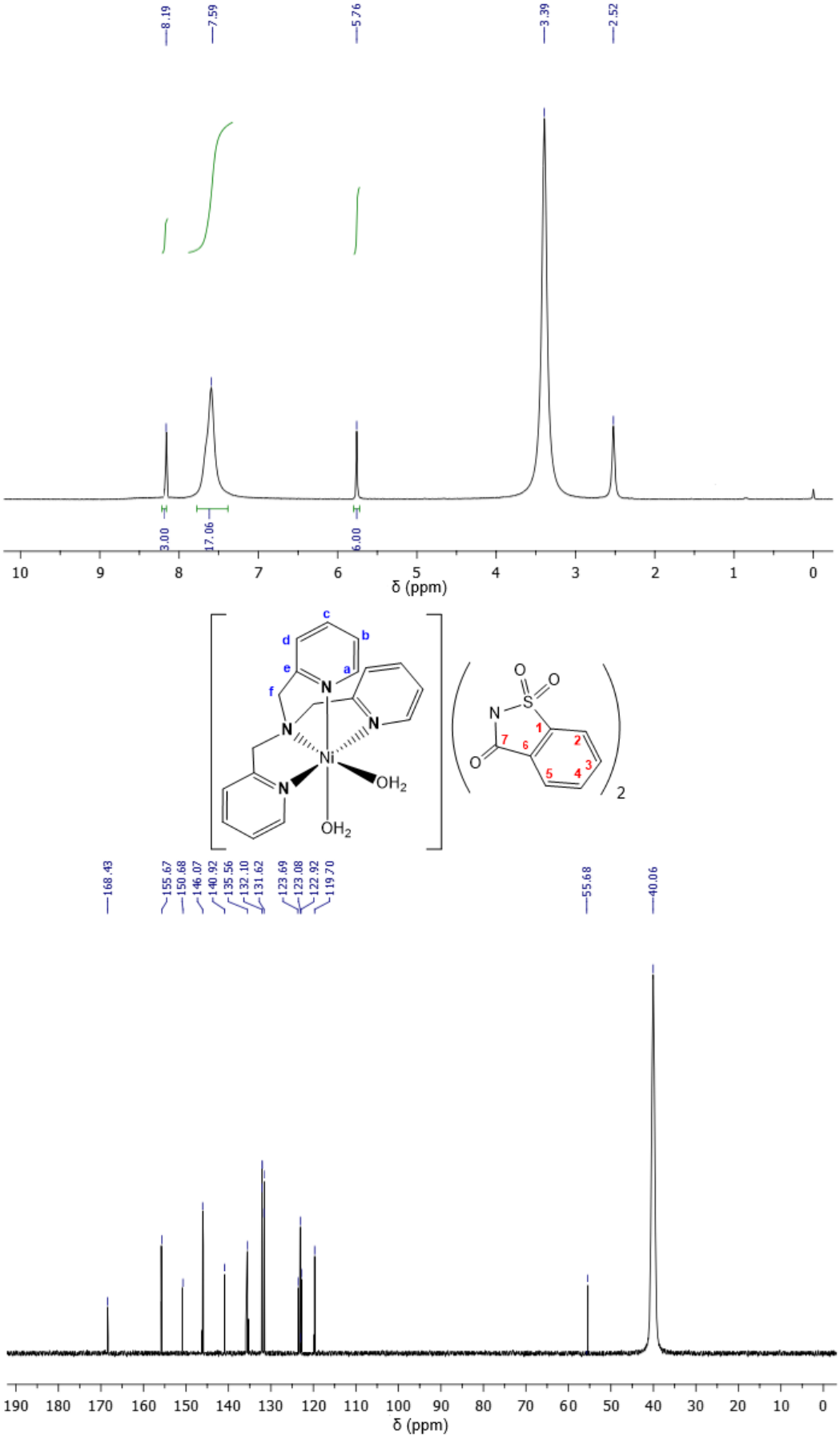

Fig. S4 continued

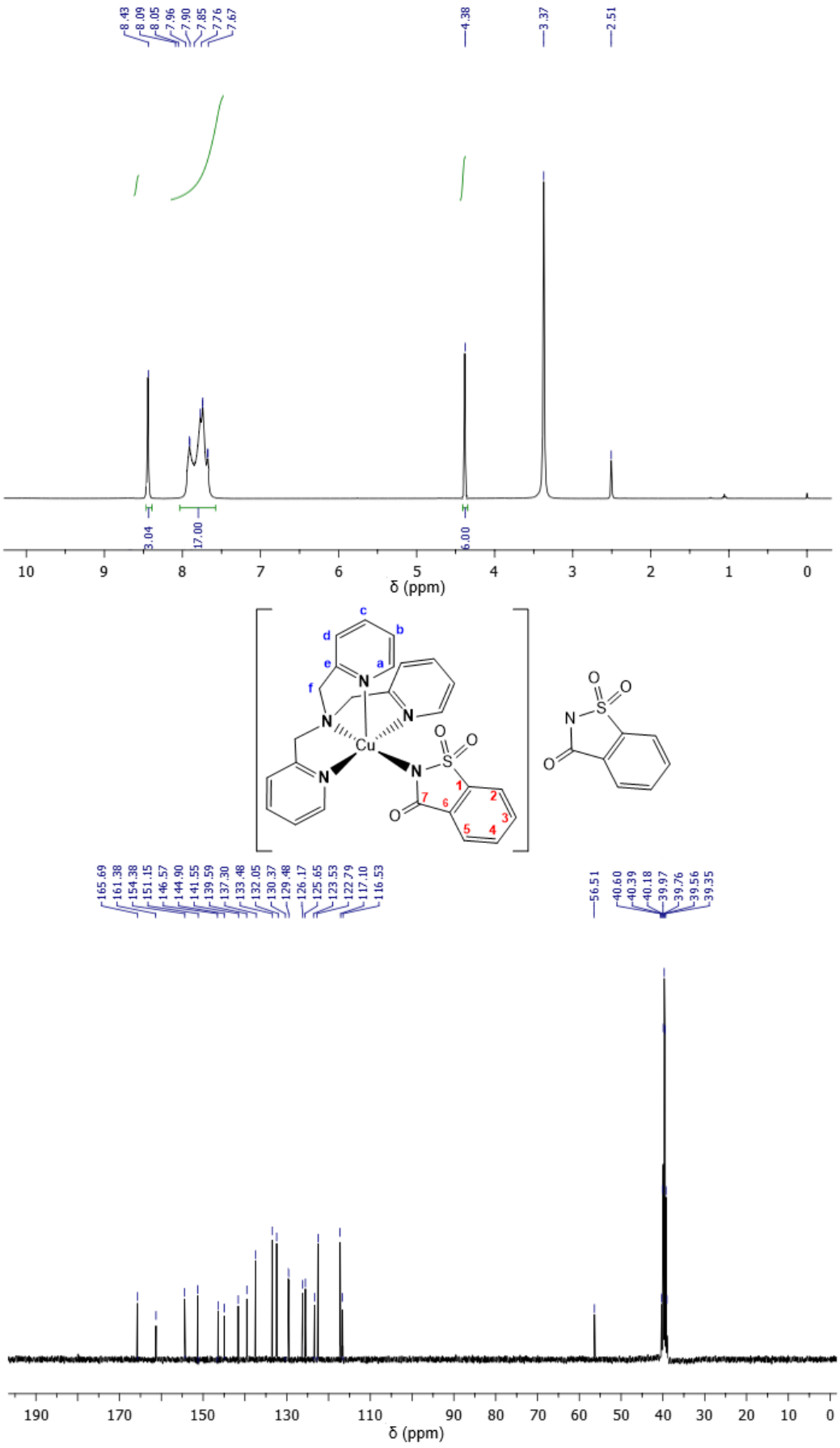

Fig. S4 continued

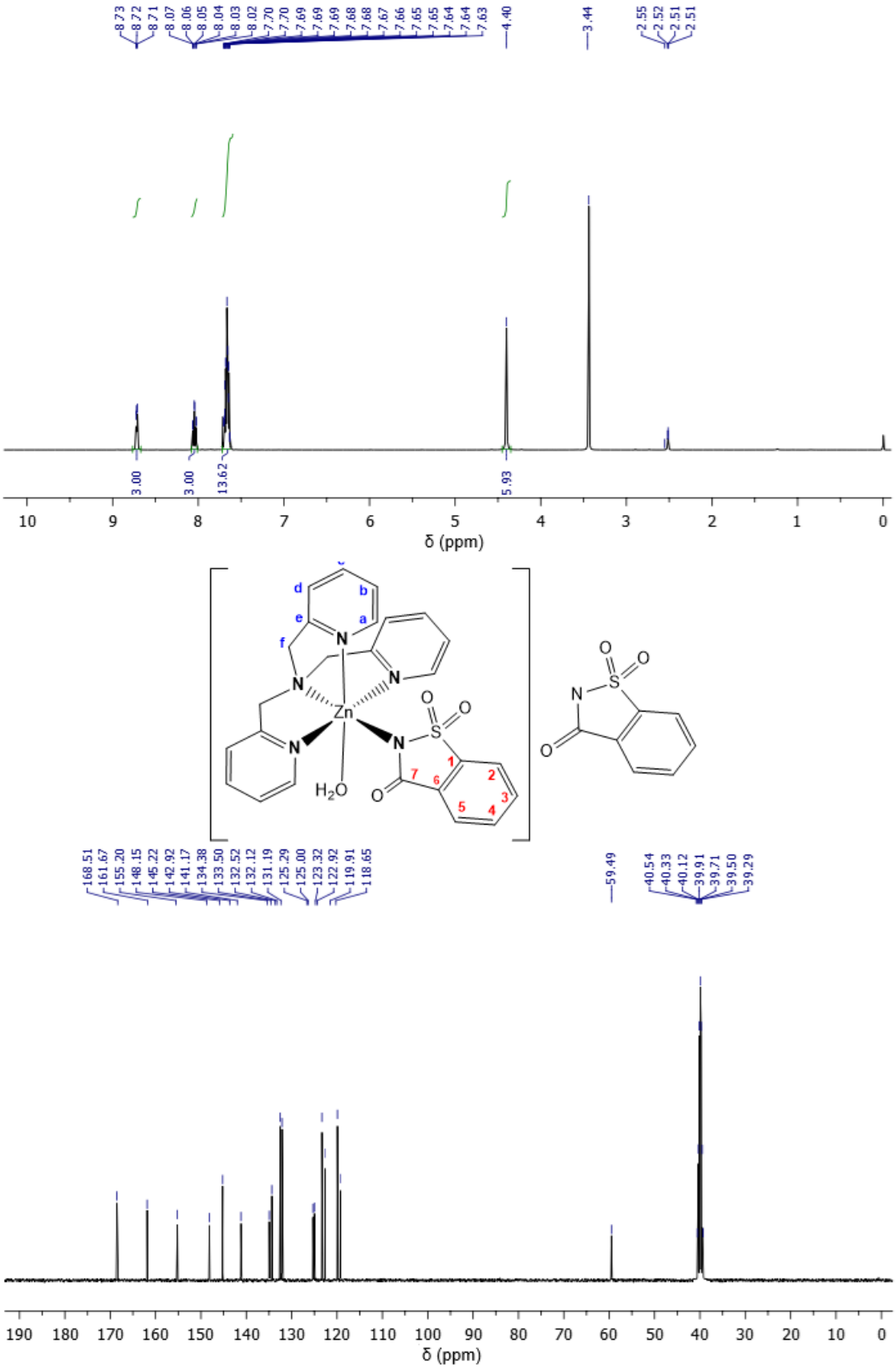

Fig. S4 ^{1}H NMR and ^{13}C spectra of metal sac complex of tpma.

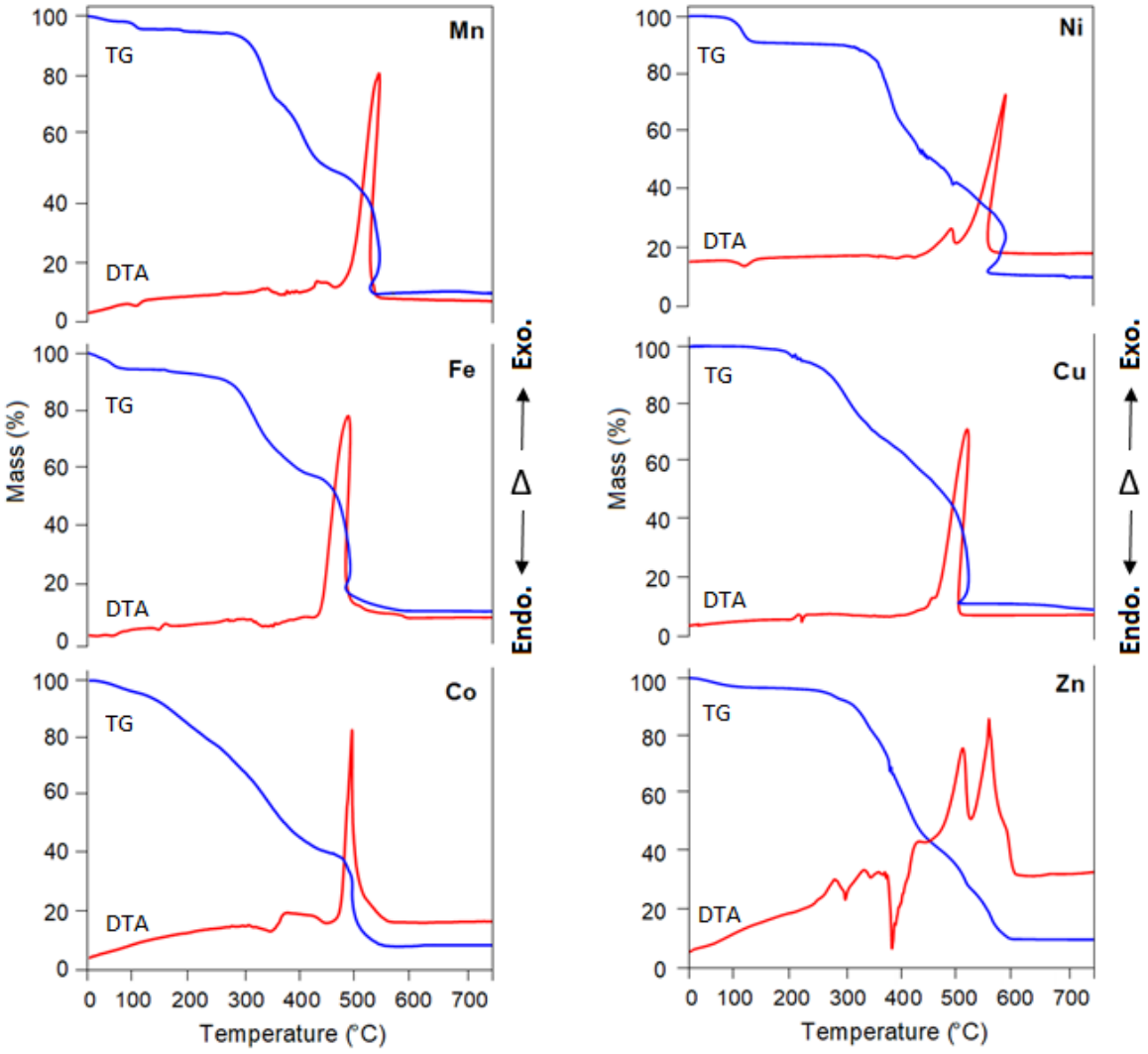

Fig. S5 Thermal analysis curves of metal sac complexes of tpma.

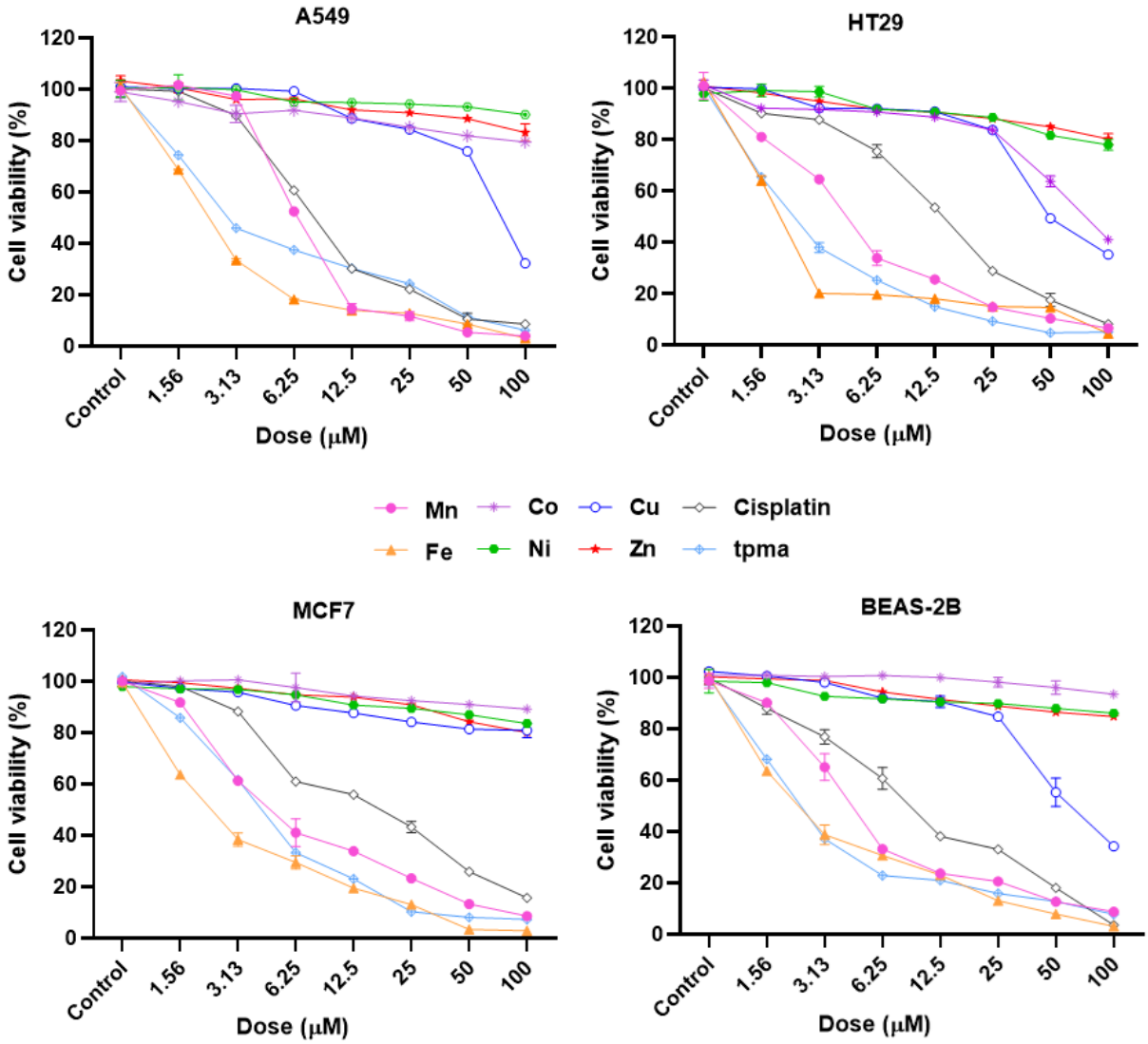

Fig. S6 The dose-response graphics for the tpma ligand, the metal sac complexes of tpma and cisplatin obtained from SRB assay, the viability of cell lines after 48 h of treatment. Results are represented as mean ± standard deviation (*n* = 3).

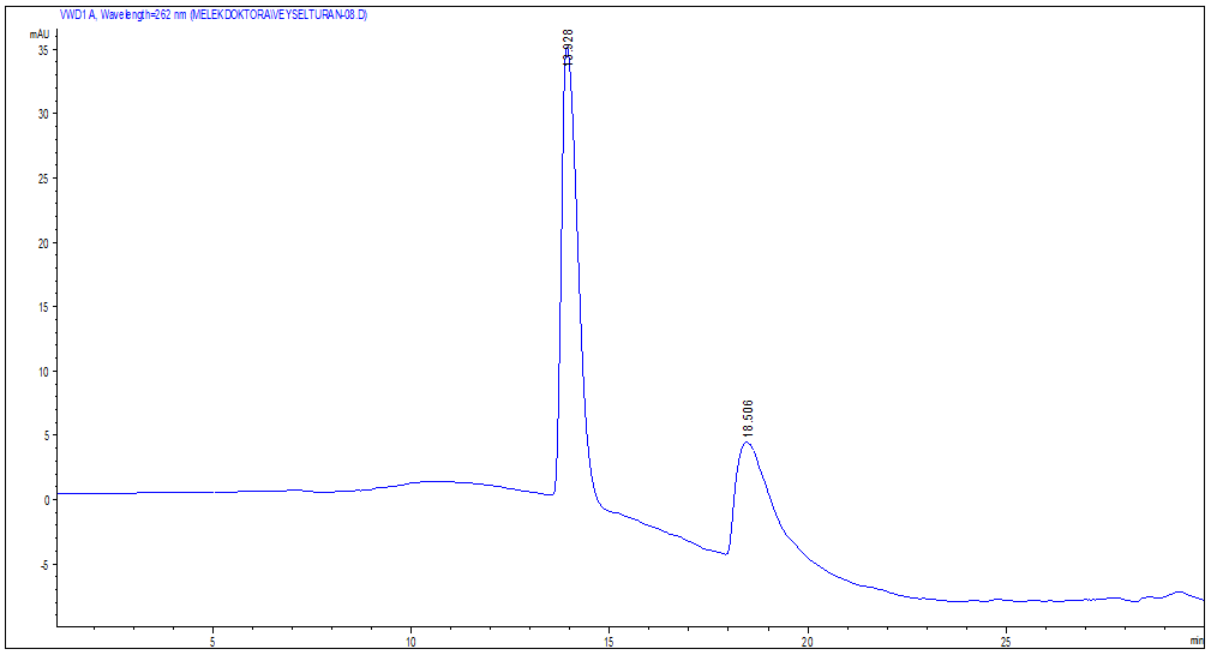

Fig. S7 The HPLC chromatogram of **Fe** (100 µM) dissolved in an aqueous solution of MeOH (1;1, v:v). The mobile phase consists of water containing 0.1% acetic acid (solvent A), and acetonitrile-water mixture with 0.1% acetic acid (v:v, 1:1, solvent B). Gradient conditions: at 0 min, 95% solvent A and 5% solvent B, and at 25 min, 10% A and 90% B. The total run time is 30 min at 262 nm.

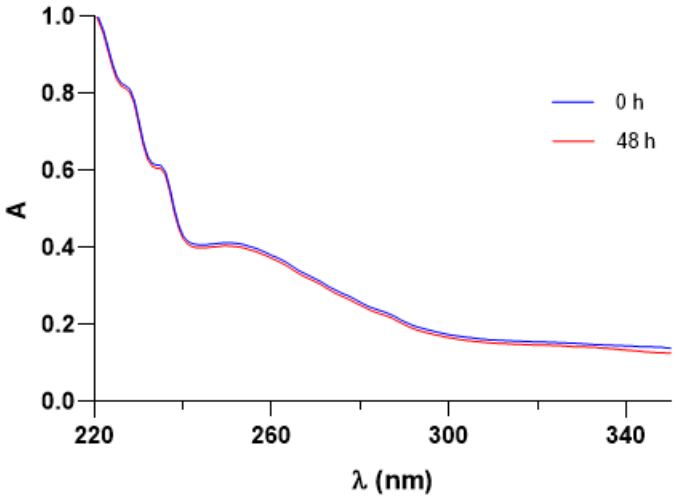

Fig. S8 Time-dependent UV-Vis spectra of 10 µM solution of **Fe** in saline.

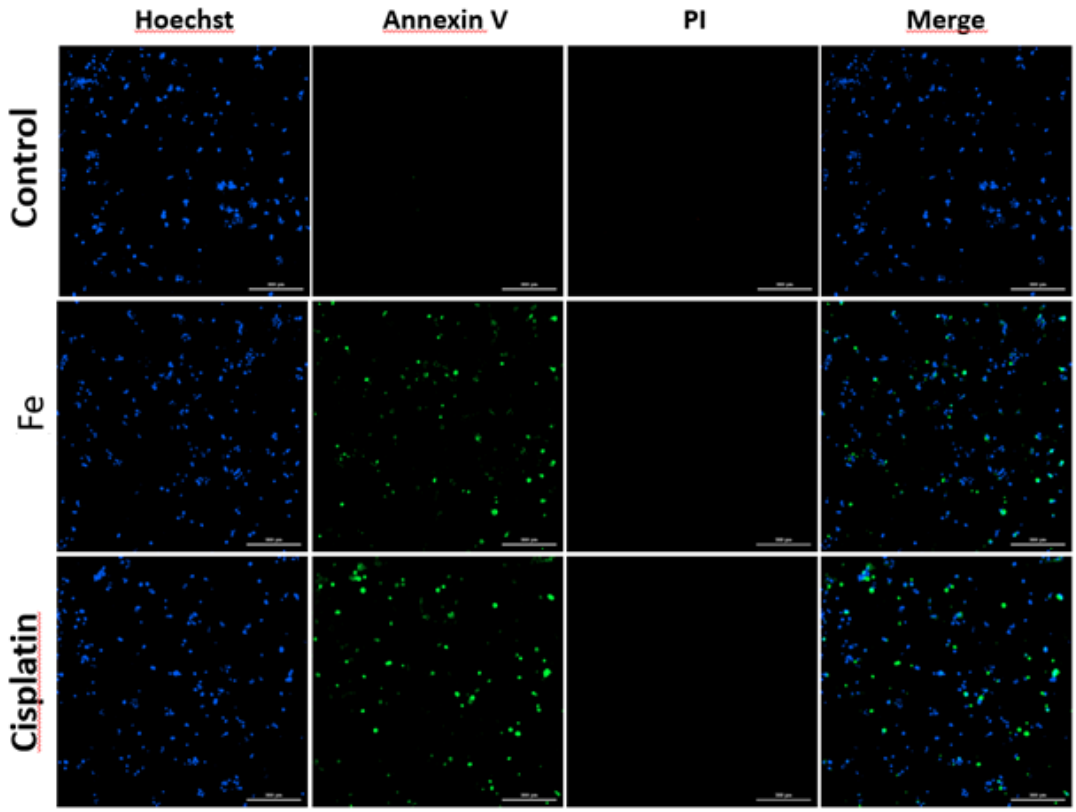

Fig. S9 Hoechst staining (blue) and Annexin V/PI staining (green/red) to detect apoptosis cells in **Fe** and cisplatin. HT29 cells were treated with IC_{75} doses of **Fe** (3 μM) and cisplatin (33.2 μM) at 12 h. Merge is Hoechst staining/Annexin V/PI staining overlay. Magnification ×10. The scale bar is 300 μm.

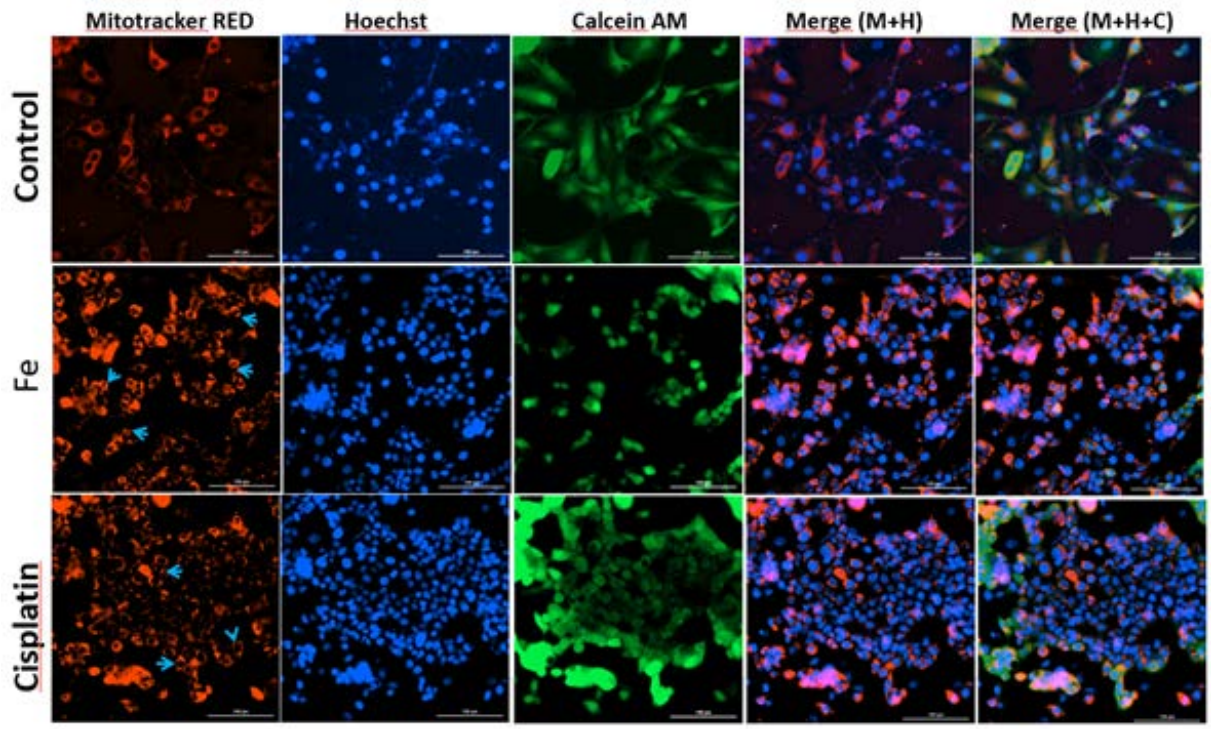

Fig. S10 HT29 cells were incubated with Mitotracker (red), Calcein AM (green), and Hoechst 33342 (blue) and imaged using an inverted fluorescent microscope (magnification ×40). Mitotracker red staining reveals that **Fe** and cisplatin-treated HT29 cells display defects in mitochondrial morphology compared to control at 12 h. Representative images show the presence of large globular aggregates (blue arrows) in **Fe** and cisplatin-treated HT29 cells. Merge is Hoechst /Calcein AM/Mitotraker RED staining overlay. The scale bar is 100 μm.

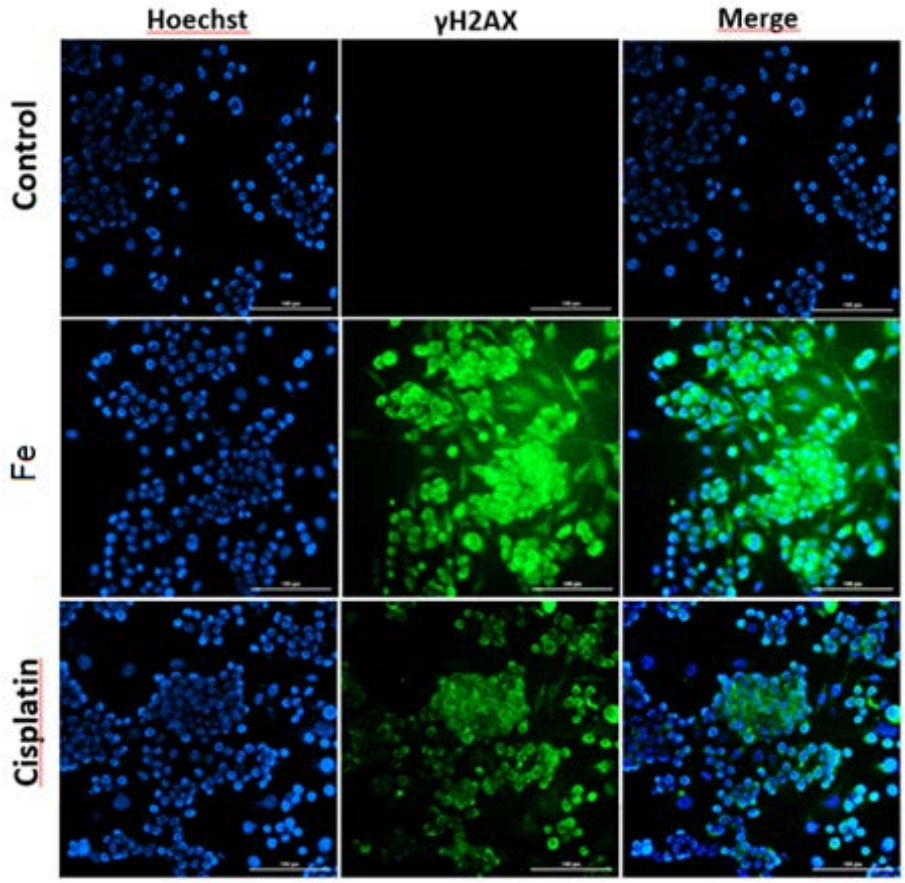

Fig. S11 Representative microscopy images from HT29 cells treated with **Fe** and cisplatin for 12h. Each treated cells were fixed and processed for γ-H2AX immunofluorescent staining. γ-H2AX staining is green; nuclei are stained with DAPI blue. γ-H2AX expression was detected in HT29 cells treated with **Fe** and cisplatin but not in control cells. Magnification: ×40. Merge is Hoechst/γ-H2AX staining overlay. The scale bar is 100 μm.